THE JOURNAL OF PHYSICAL CHEMISTRY C

ARTICLE

pubs.acs.org/JPCC

Designed Growth and Characterization of Radially Aligned Ti_5Si_3 Nanowire Architectures

Yong Zhang,[†] Dongsheng Geng,[†] Hao Liu,[†] Mohammad Norouzi Banis,[†] Mihnea Ioan Ionescu,[†] Ruying Li,[†] Mei Cai,[‡] and Xueliang Sun*[,†]

[†]Department of Mechanical and Materials Engineering, The University of Western Ontario, London, Ontario N6A 5B9, Canada

[‡]General Motors Research and Development Center, Warren, Michigan 48090-9055, United States

Supporting Information

ABSTRACT: Radially aligned and high-density Ti_5Si_3 nanowire architectures have been designedly obtained on carbon microfibers through a self-assembly growth by atmospheric pressure chemical vapor deposition. The morphology, structure, and composition of obtained nanowires have been characterized using field emission scanning electron microscopy (FESEM), X-ray diffraction (XRD), high-resolution transmission electron microscopy (HRTEM), and energy dispersive X-ray spectroscopy (EDX). The results indicate coaxial cable structure of the nanowires, featuring Ti_5Si_3 nanocore and silicon oxide nanoshell. The growth mechanism of the nanowires has been proposed as a vapor−liquid−solid (VLS) mechanism. Cyclic voltammetry measurement of the nanowires demonstrates that the Ti_5Si_3 nanowires show evident electrochemical capacitance characteristics, which may find many applications in producing electrochemical nanodevices, such as electrochemical capacitors.

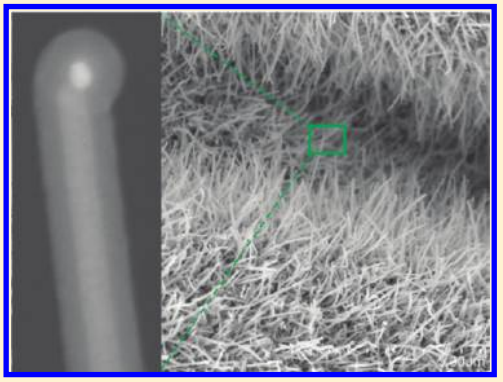

INTRODUCTION

Transition metal silicides represent an extremely broad set of refractory materials that are currently employed for many applications and have been widely investigated during the past decades.[1] With the dimensional shrinkage of conventional electronic devices, the development of nanostructured metal silicides bestows a promising pass to achieve ideal building blocks with higher device densities that the conventional semiconductor technology cannot provide.[2] Recently, some metal silicide nanowires, such as Ti,[3−8] V,[9] Cr,[10,11] Mn,[12,13] Fe,[14−18] Co,[19,20] Ni,[21,22] Cu,[23] Au,[24] Pt,[25] and Ta,[26] Y,[27] and Dy,[28] have been developed using various techniques. Among them, titanium silicides have attracted steadily increasing interest due to their relative low electrical resistivity, high stability, and low work function.[29] These unique properties make them the ideal candidates not only for electronic nanodevices but also for electrochemical nanodevices requiring high electrical conductivity and corrosion resistance. Up to date, TiSi[5,7] and $TiSi_2$[3,6,8] are among the more recently reported TiSix nanowires, while the investigation of Ti_5Si_3 nanowires is still ongoing and interesting field emission property of Ti_5Si_3 nanowires has been explored.[4] In addition, it is a crucial prerequisite to assemble nanowires directly onto a suitable substrate to form an appropriate spatial architecture for practical applications. A successfully assembled Ti_5Si_3 nanowires architecture will not only provide us opportunities to better understand the relationship between physical/chemical properties and size/dimension of the nanowires but also allow us to explore the potential applications of this spatial arrangement of the nanowires.

In this paper, we describe a simple method to synthesize highly uniform and radially aligned Ti_5Si_3 nanowires onto the carbon microfibers, using chemical vapor deposition at atmospheric pressure. The resultant hierarchical structures promise many potential applications such as catalyst electrodes, electrochemical capacitors, and other chemical nanodevices.

EXPERIMENTAL PROCEDURE

The synthesis of nanowires was carried out by a hot wall chemical vapor deposition method. The commercially available carbon paper was obtained from E-TEK, a division of De Nora North America, Somerset, NJ, and is composed of carbon microfibers of 5−10 μm in diameter. In order to grow Ti_5Si_3 nanowires onto carbon microfibers, a 1 μm thick titanium film was deposited onto carbon paper microfibers by radio-frequency (RF) magnetron sputtering using a titanium target (purity 99.99%) with high-purity argon (purity 99.999%). The chamber pressure was maintained at 4.6×10^{-3} Torr during sputtering deposition. A 5 nm thick gold layer was then sputtered onto the titanium film as catalyst. This Ti/Au-coated carbon paper substrate was moved into the middle part of a quartz tube, which was mounted horizontally inside a furnace. High-purity argon (99.999%) was first passed through the quartz tube at a rate of 400 sccm (standard cubic centimeters per minute) for 20 min to purge out the oxygen in the tube. Then the carrier gas

Received: May 29, 2011
Revised: July 7, 2011
Published: July 11, 2011

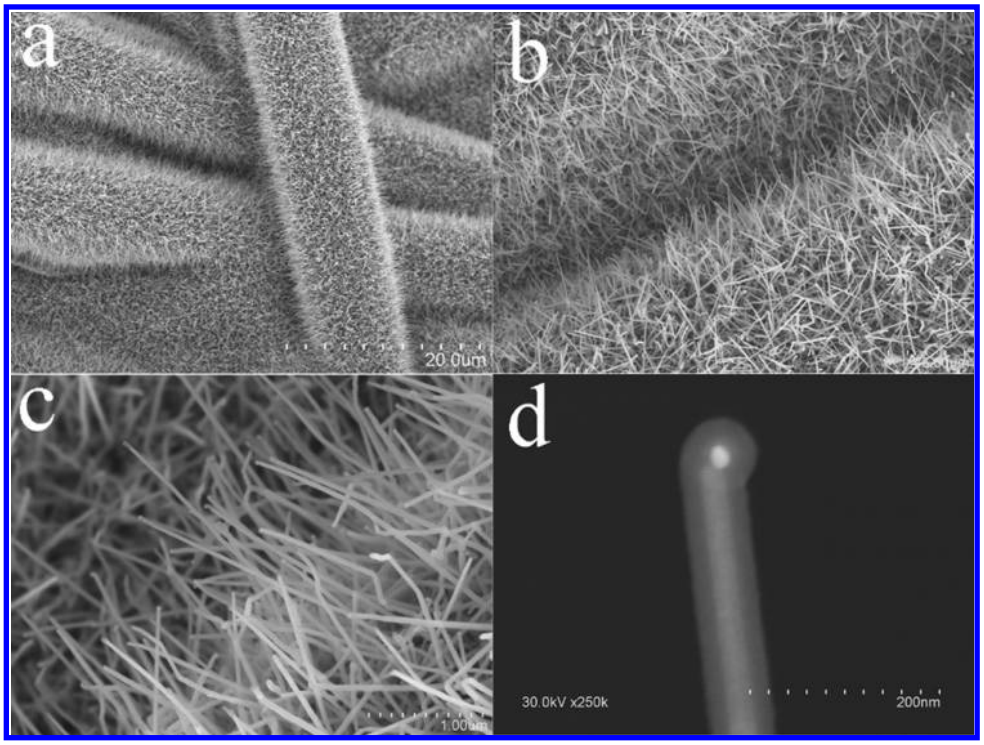

Figure 1. FESEM images of Ti_5Si_3 nanowires under different magnifications.

was switched to a mixture of Ar(220 sccm)/H_2(180 sccm), and $SiCl_4$ vapor was introduced into the system by passing pure Ar through a beaker containing liquid $SiCl_4$ as the silicon source to induce the growth of Ti_5Si_3 nanowires. The furnace was then heated to 750 °C at a heating rate of 50 °C/min and held at that temperature for 5 h before $SiCl_4$ flow was turned off. The carrier gas flow was kept on until the furnace was cooled to room temperature.

The as-synthesized product was initially examined using a Hitachi S-4800 field emission scanning electron microscope (FESEM). Additional detailed structural and compositional characterization of the 1D nanowire structures was carried out using a Bruker D8 micro X-ray diffractometer equipped with Cu Kα radiation, a Oxford INCA energy dispersive X-ray spectroscope (EDX) operated at 10 keV, a JEOL 2010 FEG transmission electron microscope (TEM) at 200 kV for high-resolution imaging, and selected area electron diffraction(SAED) determination. In order to investigate the thickness effect of silicon oxide shell on the electrochemical behavior of the nanowires, the sample was immersed in a 10% HF solution for different time to etch away the silicon oxide layer. Electrochemical behavior of the samples was evaluated with 0.5 M H_2SO_4 at room temperature using an Autolab potentiostat/galvanostat (model PGSTAT-30) scanned from −200 to 1000 mV versus a saturated calomel reference electrode (SCE) at a scanning rate of 50 mV/s.

RESULTS AND DISCUSSION

Figure 1 shows different magnification FESEM images of nanowires grown on carbon microfibers. The low-magnification SEM image indicates the successful growth of radially aligned nanowires onto carbon microfibers, as shown in Figure 1a. Higher magnification images show the aligned and highly dense nanowires totally cover the surface of carbon microfibers (Figure 1b). As shown in Figure 1c, the nanowires possess uniform diameter of 40−80 nm throughout their length, with typical length of 2−3 μm. A close-up cross section view of a single nanowire at high accelerating voltage indicates that the core−shell structure of the nanowire with a catalyst particle at the tip of nanowire, as shown in Figure 1d.

In order to further characterize the structure of produced nanowires, XRD, TEM, and HRTEM analysis were performed. Figure 2a shows the XRD pattern of the nanowires grown on the carbon microfibers. Besides the peaks of carbon substrate, two sets of diffraction peaks were detected in the product. One set of peaks can be indexed to Ti_5Si_3 (JCPDS 29-1362), and the other ones can be assigned to metal gold (JCPDS 04-0784). Figure 2b shows a low-magnification TEM image of the nanowires taken from carbon microfibers, revealing a typical core/shell structure with coaxial cable feature. To get insight into the core/shell structure of the nanowire, scrutiny of the nanowire was conducted by HRTEM. The bright field image shown in Figure 2c indicates that the core/shell structure is composed of single crystalline core and amorphous shell with the shell thickness of around 10 nm. Figure 2d clearly indicates the well-defined lattice fringe spacing of 2.55 Å, corresponding to the (020) plane of the hexagonal Ti_5Si_3 phase. Figure 3a shows a typical TEM image of a single nanowire of 40 nm in diameter, revealing an evident core shell structure of the nanowire with a catalyst particle at the tip. To acquire compositional information on the nanowire, EDX spectra were taken from the core area, shell area, and tip of the nanowire. Figure 3b shows the EDX spectrum taken from the core area of the nanowire as indicated in the area "1" of Figure 3a. Besides copper signals from the TEM grid, elements of titanium, silicon, and oxygen were exclusively detected. While the electron probe was shifted to the shell area of the nanowire, as shown in Figure 3c, signals of silicon and oxygen dominated the spectrum while peaks of titanium element significantly decreased, revealing

dx.doi.org/10.1021/jp2050096 |J. Phys. Chem. C 2011, 115, 15885–15889

a silicon oxide-rich shell of the nanowire. It should be noted here that the disturbance of the core part is hard to be screened during the EDX detection of the shell part due to the small diameter of the nanowire. Figure 3d shows the EDX spectrum taken from the nanowire tip as indicated in the area "2" of Figure 3a, gold element was shown to be the dominant element by subtracting the copper background, and signals of titanium, silicon, and oxygen were also detected. The EDX result at the nanowire tip is consistent with SEM observation and the gold peaks detected in the XRD pattern, implying the catalytic growth of the nanowire directed by gold nanoparticle. Combined with the HRTEM examination, it can be deduced that the amorphous shell is mainly composed of silicon oxide.

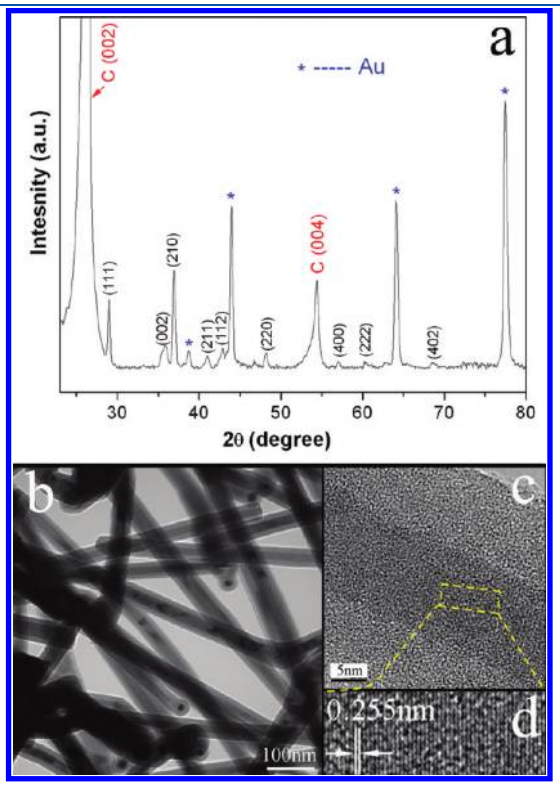

Figure 2. (a) XRD pattern, (b) low-magnification TEM image, (c) magnified TEM image, and (d) high-resolution TEM image of the Ti_5Si_3 nanowires.

Based on the SEM and TEM investigations, the growth of the Ti_5Si_3 nanowires can be ascribed to a catalytic growth process following a well-recognized VLS mechanism as illustrated schematically in Figure 4. First, a thin Au/Ti layer was sputtered on the carbon microfibers as shown in Figure 4a and put into the reaction system. After the air purge process, the system was heated to the target temperature. Then $SiCl_4$ was introduced into the reaction chamber, and active silicon atoms were generated as shown in Figure 4b. Because of low eutectic point (363 °C) of Au−Si alloy, liquid Au−Si droplets were able to be formed under the reaction temperature. The chlorine species originated from the $SiCl_4$ could react with the titanium film and generate titanium chloride vapor. While the alloy droplet became supersaturated with the absorbed elements, the formation of Au−Ti−Si system would result in the nucleation of Ti_5Si_3, and nanosized Ti_5Si_3 nuclei were generated from the liquid droplets.[30] Meanwhile, the droplets absorbed residue oxygen species in the system, and silicon oxide shell was formed around the Ti_5Si_3 core. The gold-containing catalyst could direct the anisotropic growth of the product, and nanorods were formed following a VLS growth (Figure 4c). The continuous addition of Ti, Si, and O species consequently led to the one-dimensional growth of the nanowires with core−shell structure. Finally, the Ti_5Si_3@silicon oxide core shell nanowires with uniform length and diameter were obtained as shown in Figure 4d. Further investigation is currently being undertaken to better understand the growth mechanism of the core shell structure. During our experiments, it was found that the growth of the Ti_5Si_3 nanowires was affected by various factors, such as temperature and the amount of $SiCl_4$. Generally, the density and growth rate of the nanowires increased with the temperature between 650 and 900 °C operating zone. Below 600 °C, the growth of the nanowires is totally restricted. Above 900 °C, silicon oxide nanowires are generated instead of Ti_5Si_3 nanowires. It should be noted that the

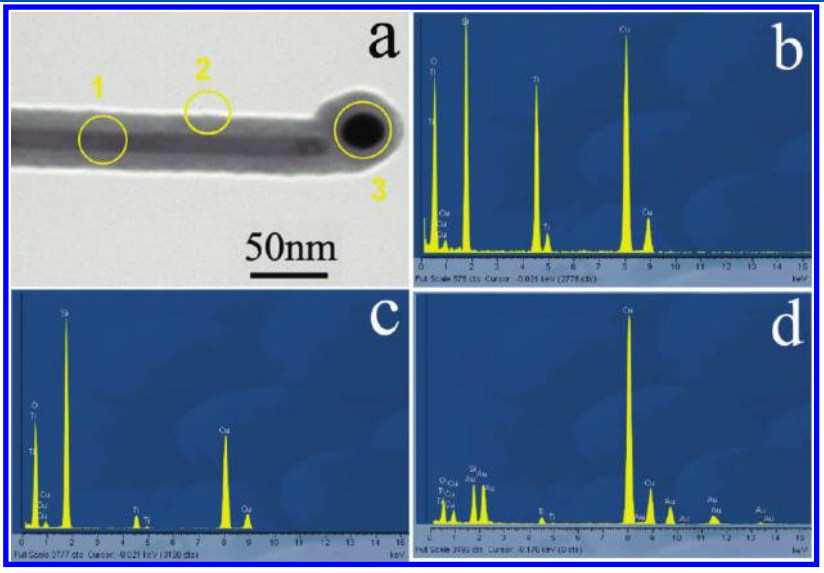

Figure 3. (a) A typical TEM image of a single Ti_5Si_3 nanowire and corresponding EDX spectra taken from (b) core area, (c) shell area, and (d) tip of the nanowire.

dx.doi.org/10.1021/jp2050096 |J. Phys. Chem. C 2011, 115, 15885–15889

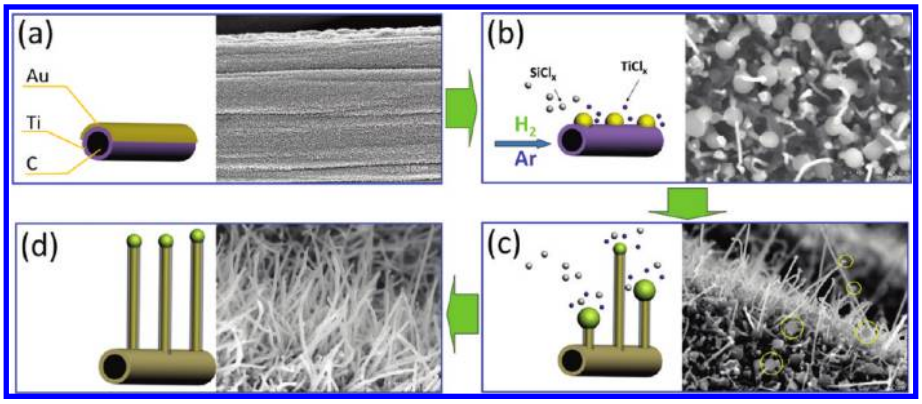

Figure 4. Schematic diagram and corresponding SEM images indicating the growth mechanism of the Ti_5Si_3 nanowires.

growth of the Ti_5Si_3 nanowires is very sensitive to the amount of $SiCl_4$ introduced. Only very short nanorods were observed at low flow rates of $SiCl_4$ possibly because of the limited silicon feeding while silicon oxide nanowires were preferably obtained in the excess of $SiCl_4$. It should be noted that thickness of the silicon oxide shell also needs to be concerned in terms of practical applications of the nanowires. During our experiments, it has been found that temperature is the crucial factor in dominating the thickness of the silicon oxide shell. We have counted and measured 100 nanowires under TEM observation and found that the average thickness of the silicon oxide shell is around 12.5 nm at the growth temperature of 700 °C, 13 nm at 750 °C, while 20.6 nm at 800 °C and 23 nm at 850 °C, which indicates the increasing thickness of the silicon oxide shell with the reaction temperature. In addition, morphology of the nanowires can be significantly affected by putting some extra titanium powder upstream from the substrate. Figures S1(a,b) and S1(c,d) show typical SEM images of the samples obtained with placing the titanium powder 1 and 2 cm upstream from the substrate. In the case of 1 cm distance, as shown in Figure S1(a), the much thinner nanowires were obtained compared to the case without introducing the extra titanium powder. Figure S1(b) shows magnified image of the nanowires with the diameter around 30 nm. With longer distance between the powder and the substrate, as shown in Figure S1(c,d), the morphology changed to a branched nanowires structure. It is still unclear to us how the extra titanium powder affects the growth of Ti_5Si_3 nanowires; we suspect that the vapor pressure of titanium source may plays an important role in dominating the morphology of the nanowires.

Recent publications have reported the superior capacitance performance of silicide nanowires and nanobelts. Therefore, we also investigated the electrochemical capacitance behavior of the Ti_5Si_3 nanowires obtained in this work. During our experiments, it has been found that the silicon oxide shell plays an important role in determining the capacitance behavior of the nanowires. Figure 5 shows normalized cyclic voltammograms of the Ti_5Si_3 samples etching in the 10% HF solution for (a) 0, (b) 120, and (c) 180 s. TEM images (see Supporting Information Figure S2) clearly show the morphology difference before and after removing the silicon oxide layer with 10% HF solution for 180s. For the as-prepared sample, an evident oxidation peak around 0.55 V can be observed in curve (a), which may due to the oxidation of the groups on the silicon oxide layer under acidic catalysis.[31] With the increasing etching time, obviously, electrochemical

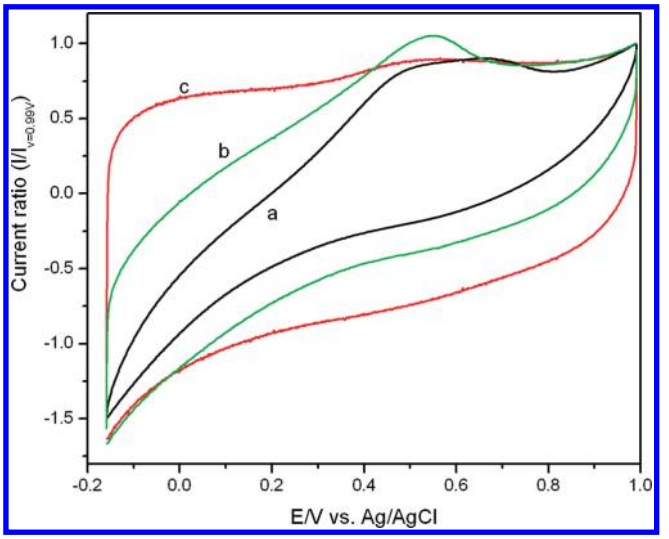

Figure 5. Normalized cyclic voltammetry of the nanowires after etching in HF solution for (a) 0, (b) 120, and (c) 180 s.

capacitance of the Ti_5Si_3 nanowires increases with the thinning of silicon oxide layer. At the etching time of 180 s, the voltammetric curve was achieved the rectangular shape, which implies the ideal capacitance behavior at relatively high scan speed of 50 mV s^{-1}. This result implies that the Ti_5Si_3 nanowires could be considered as promising material in the application of nanodevices for electrochemical energy storage.[32,33] Because of the possible loss of the nanowires during the etching procedure, it is still a challenge to calculate the exact capacity of the nanowires, and our work is continued to grow Ti_5Si_3 nanowires without or with a very thin silicon oxide layer and quantitatively calculate the capacity of the nanowires. In addition, further work evaluating the structure and electrochemical performance of the product with different morphology is underway.

CONCLUSIONS

Single crystalline Ti_5Si_3 nanowires with radially aligned architecture has been obtained on carbon microfibers based on a self-assembly growth by chemical vapor deposition at atmospheric pressure. Structure analysis indicates that the nanowires possess coaxial cable structure, featuring Ti_5Si_3 nanocore and silicon oxide nanoshell. The growth mechanism of the nanowires has

been proposed as a catalytic growth directed by gold particles base on the VLS mechanism. Cyclic voltammetry measurement of the nanowires indicates that the Ti_5Si_3 nanowires shows superior electrochemical capacitance features, which may find great potential applications in producing electrochemical nanodevices, such as fuel cell electrodes and electrochemical capacitors.

■ ASSOCIATED CONTENT

Supporting Information. SEM observation of the Ti_5Si_3 nanowires with different morpologies after adding extra titanium powder as the precursor; TEM investigation of the nanowires before and after etching treatment by HF solution. This material is available free of charge via the Internet at http://pubs.acs.org.

■ AUTHOR INFORMATION

Corresponding Author
*Tel: (1)-519-661-2111 ext 87759. Fax: (1)-519-661-3020. E-mail: xsun@eng.uwo.ca.

■ ACKNOWLEDGMENT

This research was supported by General Motors of Canada, Ontario Centres of Excellence, Natural Sciences and Engineering Research Council of Canada (NSERC), Canada Research Chair Program, Canada Foundation for Innovation, Ontario Early Researcher Award, and the University of Western Ontario. We thank Fred Pearson for fruitful discussions, structural characterization, and special support.

■ REFERENCES

(1) Lee, J.; Reif, R. *J. Electron. Mater.* **1991**, *20*, 331.
(2) Schmitt, A. L.; Higgins, J. M.; Szczech, J. R.; Jin, S. *J. Mater. Chem.* **2010**, *20*, 223.
(3) Xiang, B.; Wang, Q. X.; Wang, Z.; Zhang, X. Z.; Liu, L. Q.; Xu, J.; Yu, D. P. *Appl. Phys. Lett.* **2005**, *86*, 243103.
(4) Lin, H. K.; Tzeng, Y. F.; Wang, C. H.; Tai, N. H.; Lin, I. N.; Lee, C. Y.; Chiu, H. T. *Chem. Mater.* **2008**, *20*, 2429.
(5) Du, J.; Du, P.; Hao, P.; Huang, Y.; Ren, Z.; Han, G.; Weng, W.; Zhao, G. *J. Phys. Chem. C* **2007**, *111*, 10814.
(6) Zhou, S.; Liu, X.; Lin, Y.; Wang, D. *Angew. Chem., Int. Ed.* **2008**, *47*, 7681.
(7) Lin, H. K.; Cheng, H. A.; Lee, C. Y.; Chiu, H. T. *Chem. Mater.* **2009**, *21*, 5388.
(8) Zhou, S.; Liu, X.; Lin, Y.; Wang, D. *Chem. Mater.* **2009**, *21*, 1023.
(9) In, J.; Seo, K.; Lee, S.; Yoon, H.; Park, J.; Lee, G.; Kim, B. *J. Phys. Chem. C* **2009**, *113*, 12996.
(10) Szczech, J. R.; Schmitt, A. L.; Bierman, M. J.; Jin, S. *Chem. Mater.* **2007**, *19*, 3238.
(11) Seo, K.; Varadwaj, K. S. K.; Cha, D.; In, J.; Kim, J.; Park, J.; Kim, B. *J. Phys. Chem. C* **2007**, *111*, 9072.
(12) Zou, Z. Q.; Wang, H.; Wang, D.; Wang, Q. K. *Appl. Phys. Lett.* **2007**, *90*, 133111.
(13) Higgins, J. M.; Ding, R. H.; DeGrave, J. P.; Jin, S. *Nano Lett.* **2010**, *10*, 1605–1610.
(14) Schmitt, A. L.; Bierman, M. J.; Schmeisser, D.; Himpsel, F. J.; Jin, S. *Nano Lett.* **2006**, *6*, 1617.
(15) Quyang, L.; Thrall, E. S.; Deshmukh, M. M.; Park, H. *Adv. Mater.* **2006**, *18*, 1437.
(16) Varadwaj, K. S. K.; Seo, K.; In, J.; Mohanty, P.; Park, J.; Kim, B. *J. Am. Chem. Soc.* **2007**, *129*, 8594.
(17) Seo, K.; Bagkar, N.; Kim, S.; In, J.; Yoon, H.; Jo, Y.; Kim, B. *Nano Lett.* **2010**, *10*, 3643.
(18) Hung, S. W.; Yeh, P. H.; Chu, L. W.; Chen, C. D.; Chou, L. J.; Wu, Y. J.; Chen, L. J. *J. Mater. Chem.* **2011**, *21*, 5704.
(19) Seo, K.; Varadwaj, K. S. K.; Mohanty, P.; Lee, S.; Jo, Y.; Jung, M.-H.; Kim, J.; Kim, B. *Nano Lett.* **2007**, *7*, 1240.
(20) Hsin, C. L.; Yu, S. Y.; Wu, W. W. *Nanotechnology* **2010**, *21*, 485602.
(21) Decker, C. A.; Solanki, R.; Freeouf, J. L.; Carruthers, J. R.; Evans, D. R. *Appl. Phys. Lett.* **2004**, *84*, 1389.
(22) Song, Y.; Schmitt, A. L.; Jin, S. *Nano Lett.* **2007**, *7*, 965.
(23) Zhang, Z.; Wong, L. M.; Ong, H. G.; Wang, X. J.; Wang, J. L.; Wang, S. J.; Chen, H.; Wu, T. *Nano Lett.* **2008**, *8*, 3205.
(24) Bhatta, U. M.; Rath, A.; Dash, J. K.; Ghatak, J.; Feng, L. Y.; Liu, C. P.; Satyam, P. V. *Nanotechnology* **2009**, *20*, 465601.
(25) Luo, J.; Zhang, L.; Zhu, J. *Adv. Mater.* **2003**, *15*, 579.
(26) Chueh, Y.-L.; Ko, M.-T.; Chou, L.-J.; Chen, L.-J.; Wu, C.-S.; Chen, C.-D. *Nano Lett.* **2006**, *6*, 1637.
(27) Zeng, C. G.; Kent, P. R. C.; Kim, T. H.; Li, A. P.; Weitering, H. H. *Nature Mater.* **2008**, *7*, 539.
(28) Ouyang, W. J.; Shinde, A.; Zhang, Y. N.; Cao, J. X.; Ragan, R.; Wu, R. Q. *ACS Nano* **2011**, *5*, 477.
(29) Murarka, S. P.; Fraser, D. B. *J. Appl. Phys.* **1980**, *51*, 350.
(30) Wolffenbutte, R. F. *Sens. Actuators, A* **1997**, *62*, 680.
(31) Szunerits, S.; Coffinier, Y.; Janel, S.; Boukherroub, R. *Langmuir* **2006**, *22*, 10716.
(32) Du, J.; Ren, Z. D.; Tao, K. Y.; Hu, A. H.; Hao, P.; Huang, Y. F.; Zhao, G. L.; Weng, W. J.; Han, G. R.; Du, P. Y. *Cryst. Growth Des.* **2008**, *8*, 3543.
(33) Zhang, H. L.; Li, F.; Liu, C.; Cheng, H. M. *Nanotechnology* **2008**, *19*, 165606.